Ionic Interactions Play a Role in the Regulatory Mechanism of Scallop Heavy Meromyosin

M. Nyitrai,*§ W. F. Stafford,† A. G. Szent-Györgyi,‡ and M. A. Geeves*

*Department of Biosciences, University of Kent at Canterbury, Canterbury, Kent, United Kingdom; †Boston Biomedical Research Institute, Watertown, Massachusetts; ‡Rosenstiel Basic Medical Sciences Research Center, Brandeis University, Waltham, Massachusetts; and §Research Group for Fluorescence Spectroscopy, Office for Academy Research Groups Attached to Universities and Other Institutions, Department of Biophysics, Faculty of Medicine, University of Pécs, Pécs, Hungary

ABSTRACT   Heavy meromyosin from scallop (scHMM) striated muscle is regulated by calcium binding to the essential light chain. The regulation can be modeled with a calcium-dependent equilibrium between *on* and *off* scHMM conformations. The observed rate constant for mant-ADP dissociation from scHMM is calcium dependent, and we show here that it can be used to define the equilibrium constant (K_{eq}) between *on* and *off* conformations. The data show that K_{eq} is markedly ionic strength dependent, with high salt ($\geq$200 mM) abolishing the *off* state even in the absence of calcium and low salt ($<$50 mM) favoring the *off* state even in the presence of calcium. Debye-Huckel plots of the equilibrium constant (K_{eq}) for the *on* and *off* forms gave parallel slopes (5.94 $\pm$ 0.33 and 6.36 $\pm$ 0.17 $M^{-0.5}$) in the presence and absence of calcium. The presence of an equilibrium mixture of two conformations was confirmed by sedimentation data and the effects of ADP, calcium and ionic strength were in qualitative agreement. Thus scHMM exists in two conformations that can be distinguished in sedimentation profiles and by the rate of release of mant-ADP. Increasing salt concentrations biases the system toward the *on* state, suggesting a role for ionic interactions in stabilizing the *off* state.

INTRODUCTION

The regulation of molluscan myosins is achieved by the direct binding of calcium to the essential light chain of the regulatory domain (Chantler and Szent-Györgyi, 1980, 1999). Whereas both the full-length myosin and the double-headed heavy meromyosin (HMM) preserve the regulatory mechanisms, the Mg-ATPase activity of the single-headed subfragment-1 (S1) is calcium independent. Full regulation appears to require the presence of an intact junction between the two heads formed by a stable coiled-coil region and may involve direct interactions between the two heads (Kalabokis and Szent-Györgyi, 1997).

In addition to calcium, the binding of nucleotides can also play an important role in regulating the activity of scHMM heads (Kalabokis and Szent-Györgyi, 1997; Jackson and Bagshaw, 1988a; Nyitrai et al., 2002). Based on the results of detailed rapid kinetic experiments, we recently proposed that the calcium-mediated regulation of the scallop HMM could be described by a cooperative kinetic model (Nyitrai et al., 2002). The model assumes that scHMM can exist in two conformations—the *on* and *off* conformations—and that the Mg-ATPase activity of the *on* state is more than 50× greater than that of the *off* conformation. Under equilibrium conditions, the transition between the *on* and *off* states is rapid, and the dynamic equilibrium between the conforma-

tions is controlled by the binding of calcium and nucleotides. Calcium binding favors the *on* state, whereas the binding of ADP to the nucleotide-binding pocket shifts the equilibrium toward the *off* conformation. The kinetic results also suggested that in the *off* conformation only one of the scHMM heads is able to bind ADP.

In the absence of actin, the phosphate release is the rate-limiting step in the ATPase cycle. However, the rate constant for dissociation of the bound ADP was also found to be calcium dependent (Jackson and Bagshaw, 1988a,b; Nyitrai et al., 2002). The dissociation rate constant observed in the presence of calcium (15 s^{-1}) was reduced by a factor of ~50 in the absence of calcium, to 0.3 s^{-1} at 100 mM KCl. Both kinetic and equilibrium methods suggested that the interaction of scHMM with nucleotides was influenced by the ionic strength. The dissociation rate constants for ADP release measured at 100 mM KCl (0.3 s^{-1}) (Nyitrai et al., 2002) was reduced by a factor of ~10–30 at 20 mM KCl to 0.01–0.03 s^{-1} (Jackson and Bagshaw, 1988a,b). Similarly, the Mg-ATPase activity in the presence of calcium and the calcium sensitivity of the ATPase were found to be ionic strength dependent in steady-state assays (Kalabokis and Szent-Györgyi, 1997; Wells et al., 1985). At low ionic strength the steady-state Mg-ATPase activity of scHMM increased 10- to 15-fold upon calcium binding to the essential light chain. At very high ionic strength (0.5 M KCl), the calcium regulation was abolished, but the ATPase activity was increased relative to that at low ionic strength.

The structural differences between the *on* and *off* conformations are not understood. The interpretation of sedimentation experiments implicated two distinct structural states of the scHMM. In one of the conformations the heads were up relative to the tail, and could rotate independently of

---

each other, whereas the other conformational state contained the heads in the down conformation (Stafford et al., 2001).

Smooth muscle myosin HMM appears to have some similarities to the regulatory mechanism of scallop HMM (Trybus, 1991) and like scHMM can bind only one ADP with high affinity in the *off* state (Berger et al., 2001; although see also Ellison et al., 2002). For the smooth muscle myosin, the transition from the *on* to the *off* conformation involves the formation of an asymmetric structure in which the two heads interact (Wendt et al., 2001).

In the present work we investigated the ionic strength dependence of the mechanism of regulation of scHMM. We propose that the *on/off* equilibrium involves charge-to-charge interactions between the two heads and is therefore sensitive to the ionic strength of the medium. In support of this hypothesis, we demonstrate that the ADP release from scHMM is ionic strength dependent and is compatible with salt affecting the equilibrium between the two conformations with very different rates of ADP release. To corroborate this argument we show that sedimentation of scHMM is consistent with an equilibrium mixture of two conformations, and the effects of ADP, calcium, and ionic strength on the equilibrium position are in qualitative agreement with the kinetic results.

MATERIALS AND METHODS

HMM preparation and characterization

HMM was prepared from 4–5 g striated scallop muscle myosin (*Argopecten irradians*) according to Stafford et al. (2001). The scHMM was routinely checked by measuring its Mg-ATPase activity in the absence of actin using the coupled assay method (Kalabokis and Szent-Györgyi, 1997). The turnover rate per scHMM head was in the range of 0.32–0.36 s^{-1} in the presence of calcium and the calcium sensitivity, i.e., (ATPase^{+Ca} − ATPase^{-Ca}) × 100/ATPase^{+Ca}, of the preparations was between 85% and 92%. The samples used in the kinetic assays were heterogeneous, consisting of 40% short and 60% long molecules that differed in tail length by 20 nm. Differences in tail lengths did not affect ATPase activity or calcium sensitivity (Stafford et al., 2001).

Kinetic experiments

All experiments were carried out at 20°C in a standard buffer of 20 mM MOPS, pH 7.0, 5 mM MgCl$_2$, and either 100 μM EGTA or 100 μM CaCl$_2$, with additional KCl to adjust to the desired ionic strength. When measurements were recorded as a function of pCa, the calcium concentration was buffered by the addition of the appropriate amount of 2 mM EGTA and 2 mM Ca-EGTA (Harrison and Bers, 1987). Fluorescence transients were recorded with a standard Hi-Tech SF-61DX2 stopped-flow spectrophotometer. Mant-ADP fluorescence was excited at 365 nm, using a 75 W Xe/Hg lamp and monochromator. Fluorescence emission was monitored through a KV389 cutoff filter. The concentrations used to describe the experimental conditions are those established after mixing the reactants in the stopped-

flow (dilution by 2, 1:1 mixing). The kinetic parameters obtained were interpreted in terms of the seven-step Bagshaw-Trentham mechanism of the myosin ATPase (see Scheme 1; see also Bagshaw and Trentham, 1974).

The measured mant-fluorescence amplitudes (A_m) were analyzed with:

$$A_{cor} = A_m \times [mant]_{total}. \tag{1}$$

The calculated amplitudes are directly proportional to the concentration of the bound mant-nucleotide (Nyitrai et al., 2002) and the corrected values (A_{cor}, in arbitrary units) are presented throughout the article.

Sedimentation studies

Sedimentation velocity experiments were carried out on a Beckman Instruments Optima XL-I Analytical Ultra-centrifuge equipped with Rayleigh optics and analyzed as described earlier (Stafford et al., 2001). Protein concentrations were typically in the range 0.1–1.0 mg/ml. All protein solutions were dialyzed against their respective buffers; dialysates and buffers were adjusted identically for different conditions. Runs were performed at 20°C and 50,000 rpm. Sedimentation coefficient values were taken from the peak positions of the $g(s^*)$ plots and were corrected for density and viscosity to standard condition of water at 20°.

RESULTS

Working hypothesis

Our working hypothesis is based on measurements of the calcium dependence of the rate constant for mant-ADP dissociation from scHMM (k_{+6}). This was measured previously at 100 mM KCl (Nyitrai et al., 2002) and is presented in Fig. 1. The analysis of the data with the Hill equation showed that k_{obs} changed between its extreme values of 0.3 s^{-1} and 15 s^{-1} with half-saturation at 0.78 ± 0.03 μM free calcium and a Hill coefficient of 1.9 ± 0.1. The simplest interpretation of the data is that the protein can exist in two conformations, which are in rapid equilibrium on the timescale of ADP release and that addition of calcium shifts the equilibrium between the two conformations. The *off* state has a slow rate constant for ADP release ($^{off}k_{+6}$) and the *on* state a fast rate constant of ADP release ($^{on}k_{+6}$) (Scheme 2).

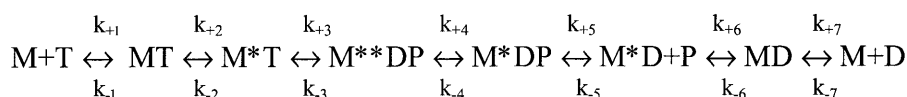In this model, the values of the observed rate constants are defined by

$$k_{obs} = {^{on}}k_{+6}\alpha[scHMM]_{total} + {^{off}}k_{+6}(1-\alpha)[scHMM]_{total} \tag{2}$$

and

$$K_{eq} = [^{on}scHMM]/[^{off}scHMM] = \alpha/(1-\alpha), \tag{3}$$

where α is the fraction of the total scHMM heads in the *on* conformation. In support of this interpretation we previously showed that the transition between the *on* and *off* conformations in the presence of ADP occurred faster than 150 s^{-1} (Nyitrai et al., 2002).

$$M+T \overset{k_{+1}}{\underset{k_{-1}}{\leftrightarrow}} MT \overset{k_{+2}}{\underset{k_{-2}}{\leftrightarrow}} M^*T \overset{k_{+3}}{\underset{k_{-3}}{\leftrightarrow}} M^{**}DP \overset{k_{+4}}{\underset{k_{-4}}{\leftrightarrow}} M^*DP \overset{k_{+5}}{\underset{k_{-5}}{\leftrightarrow}} M^*D+P \overset{k_{+6}}{\underset{k_{-6}}{\leftrightarrow}} MD \overset{k_{+7}}{\underset{k_{-7}}{\leftrightarrow}} M+D$$

SCHEME 1 The seven-step kinetic scheme for the interaction of myosin with nucleotides (Bagshaw and Trentham, 1974). In the model, the forward (k_{+i}) and reverse (k_{-i}) rate constants are presented.
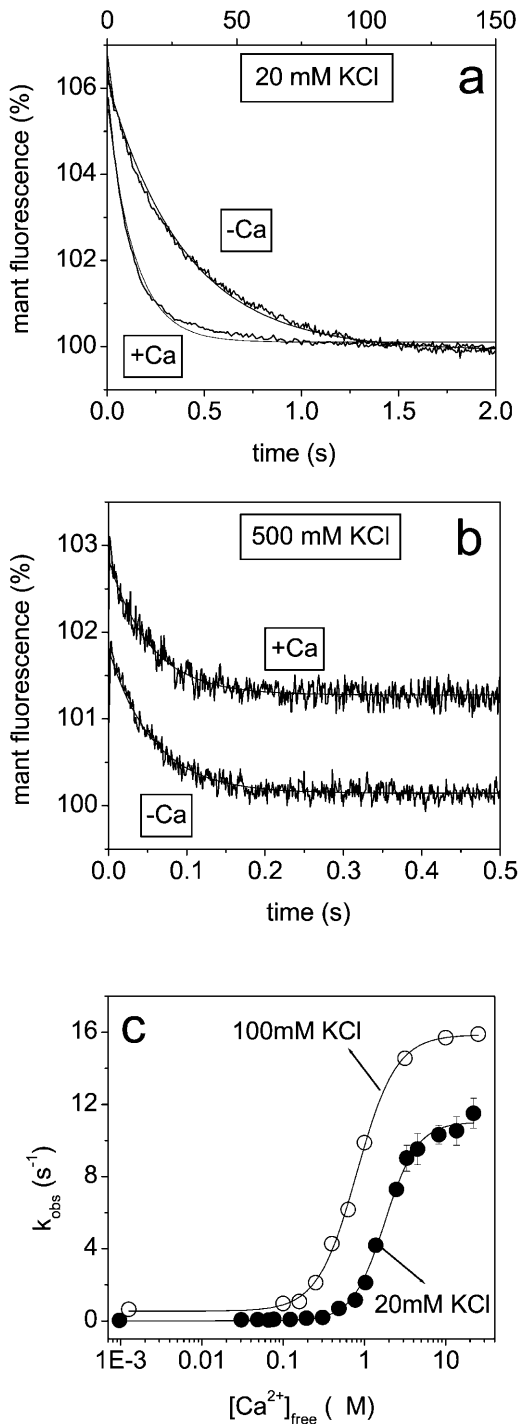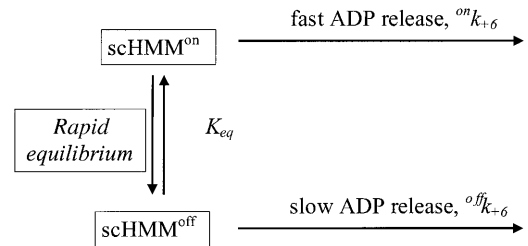
SCHEME 2   The kinetic scheme for the dissociation of ADP from scHMM.

To test if this model was valid across a range of salt concentrations we repeated the mant-ADP dissociation experiments at 20 mM KCl and 0.5 M KCl. As in the previous work, mant-ADP (10 μM) was displaced from scHMM by addition of excess of ATP (300 μM) and the decrease in mant-fluorescence was recorded (Fig. 1, a and b). At 20 mM KCl the fluorescence decrease was well-described by a single exponential at high [calcium] but became biphasic as the [calcium] was reduced (Fig. 1 a). At low calcium the k_{obs} of the faster component was $\sim$8.0 s^{-1} and had an amplitude of $\sim$15–20% of the total signal change, and both k_{obs} and its relative contribution to the total amplitude were independent of [calcium]. This is consistent with previous studies that showed the presence of 15–20% of unregulated HMM which behaves as though it is always on. The k_{obs} of the slower component was dependent upon the calcium concentration as shown in Fig. 1 c. The k_{obs} values at 20 mM KCl were all lower than those at 0.1 M KCl but still showed a similar calcium dependence (Fig. 1 c). Analysis by the Hill equation gave a Hill coefficient of 2.2 $\pm$ 0.7 and half-saturation at 1.8 $\pm$ 0.4 μM calcium. The cooperativity of the transition shows little change but there was a weakening of the calcium affinity from 0.78 μM at 0.1 M KCl. The model of Scheme 2 therefore remains valid at low ionic strength.

The model was not valid at high ionic strength. At 0.5 M KCl the decrease in fluorescence (1.6%) could be described by a single exponential (Fig. 1 b) and the k_{obs} for mant-ADP release was calcium independent (20.3 s^{-1}, +Ca; and 19.0 s^{-1}, −Ca). Thus the scHMM appears to be in the on state and removal of calcium did not produce the off conformation. This is consistent with previous studies that showed a high ATPase activity and loss of the calcium regulation at high ionic strength (Kalabokis and Szent-Györgyi, 1997). These studies also showed that calcium regulation was increased at low ionic strength but the low salt reduced ATPase activity. We proposed that the lower k_{obs} values for mant-ADP release at low ionic strength could represent a small shift in equilibrium toward the off state even in the presence of calcium.

FIGURE 1   The calcium dependence of the mant-ADP dissociation rate constant. Scallop HMM (0.5 μM) and 10 μM mant-ADP were mixed with large excess of ATP (300 μM). Mant-fluorescence transients at 20 mM KCl, a, or at 500 mM KCl, b, in the presence or absence of calcium (*indicated on the figures*). (*a*) +Ca: single-exponential fit; k_{obs} = 7.2 s^{-1}; 5.6% amplitude. −Ca: double-exponential fit; k_{obs} = 8.0 s^{-1} and 0.03 s^{-1}; 0.7% and 6.3% amplitudes. (*b*) +Ca: single-exponential fit; k_{obs} = 20.3 s^{-1}; 1.57% amplitude. −Ca: k_{obs} = 19.0 s^{-1}; 1.66% amplitude. The +Ca transient is shown with an offset to provide clearer presentation. (*c*) The calcium dependence of the mant-ADP dissociation rate constant. The solid lines represent the results of Hill analysis, which gave half-saturation calcium

concentration of 1.8 $\pm$ 0.4 μM and Hill coefficient of 2.2 $\pm$ 0.7 at 20 mM KCl. The results measured at 100 mM KCl (*empty circles*) are from Nyitrai et al. (2002), with Hill parameters of 0.78 μM and 1.9 at 100 mM KCl.

To test this idea we examined the ionic strength dependence of the k_{obs} values in the presence and absence of calcium. The results of such a measurement are shown in Fig. 2 a together with a similar measurement using scS1, which lacks any calcium regulation of its ATPase activity. At 0.5 M KCl the k_{obs} values were similar for scS1 (20.4 s^{-1}) and scHMM, and were calcium independent, again consistent with only the presence of the on state of the proteins. In the case of scS1 the k_{obs} value decreased as the salt concentration was reduced to a limiting value of 11 s^{-1} at zero [KCl] indicating the intrinsic ionic strength dependence of mant-ADP release from the on state of the proteins. In the case of scHMM the k_{obs} values showed a more marked reduction as the ionic strength was reduced to a limiting value of 2 s^{-1} in the presence of calcium and to 0.01–0.03 s^{-1} in the absence of calcium for 0 mM KCl. In our working hypothesis this salt dependence is the result of the ionic strength dependence of the on-off equilibrium constant. If the model of Scheme 2 is correct, then if we know the intrinsic value of the rate constant of mant-ADP release from the on state (provided by the values for S1) and assume that the rate constant of mant-ADP release from the off state is negligible, we can calculate the value of K_{eq} (Eq. 1 and 2). This was done for the data both in the presence and absence of calcium and the results are presented in a Debye-Huckel plot in Fig. 2 b. The Debye-Huckle plot shows the $+$Ca and $-$Ca data as two almost parallel lines with slopes of 5.94 $\pm$ 0.33 and 6.36 $\pm$ 0.17 M$^{-0.5}$, respectively. This is consistent with a common mechanism for the effect of salt in the presence and absence of calcium. The limiting values of the equilibrium constant (K_{eq}) at zero ionic strength are 0.14 in the presence of calcium and 10^{-4} in the absence of calcium. The calculated values of K_{eq} at 20 mM KCl and 0.1 M KCl are given in Table 2.

The on/off equilibrium in the absence of ADP

In our previous study we demonstrated that the rate of mant-ADP binding to scHMM could be used to estimate the fraction of scHMM in the off and on conformations in

nucleotide-free states. The binding of mant-ADP to scHMM can be followed by the increase of mant-fluorescence. At 100 mM KCl the observed reaction for mant-ADP binding to scHMM was single exponential in the presence of calcium consistent with a single population of on state heads. In the absence of calcium the transients were described by two exponentials. The faster phase was attributed to the scHMM in on conformation, whereas the slower phase reflects the binding of mant-ADP to the off heads. The ratio of the two forms was estimated to be 7:4 in favor of the on conformation from amplitudes. This experiment was repeated here in 20 mM KCl. Fig. 3, a and b, show the mant-fluorescence traces obtained in the experiments, which were two-exponential in either the presence or absence of calcium, suggesting the presence of both on and off conformations at 20 mM KCl even in the presence of calcium. The results of the two-exponential fits are presented in Fig. 3, c and d.

In the presence of calcium the k_{obs} vs. [mant-ADP] plot was linear for both phases and gave an apparent second-order rate constant of 9 $\times$ 10^5 M^{-1}s^{-1} for the faster phase and 2.4 $\times$ 10^5 M^{-1}s^{-1} for the slower phase (Fig. 3 c). The intercept was ~15 s^{-1} for the faster phase and 2 s^{-1} for the slower phase, although this latter value was not well-defined. The mant-ADP concentration dependence of the amplitudes was fitted to hyperbolae and gave half-saturation at 18 μM mant-ADP for the faster phase. The half-saturation mant-ADP concentration gives an estimation of the dissociation equilibrium constant for ADP binding to the on state (K_6K_7). For the slower phase, half-saturation occurred below 2 μM mant-ADP, giving an upper limit for K_6K_7 for the off state. The maximum amplitudes values of 1.1 and ~0.03 were resolved for the faster and slower phases, respectively. At saturation the maximum amplitudes are proportional to the bound [mant-ADP] and the fast and slow phase amplitudes provide an estimate of the contribution of on and off states after correcting for the observation that scHMM can bind two mant-ADP in the on, and only one mant-ADP in the off conformation (see Fig. 5, and Nyitrai et al., 2002). Although the presence of scHMM heads in the off conformation was
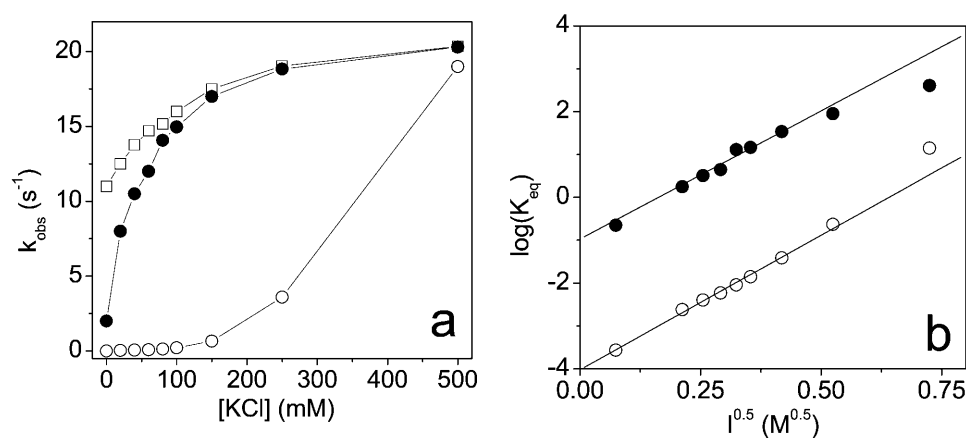

FIGURE 2 The ionic strength dependence of the mant-ADP dissociation rate constant. Scallop HMM (0.5 μM) or scS1 (0.5 μM) and 10 μM mant-ADP were mixed with ATP (300 μM) at different [KCl]. (a) Dependence of k_{obs} values on the [KCl] for scS1 (*empty squares*) and scHMM in the presence (*filled circles*) or absence (*empty circles*) of calcium. (b) The Debye-Huckel plots (log(K_{eq}) vs. $I^{0.5}$) in the presence (*filled circles*) and absence (*empty circles*) of calcium. The slopes were 5.94 $\pm$ 0.33 and 6.36 $\pm$ 0.17 M$^{-0.5}$ and the value of K_{eq} at infinite dilution was found to be 0.14 and 10^{-4} in the presence and absence of calcium, respectively.
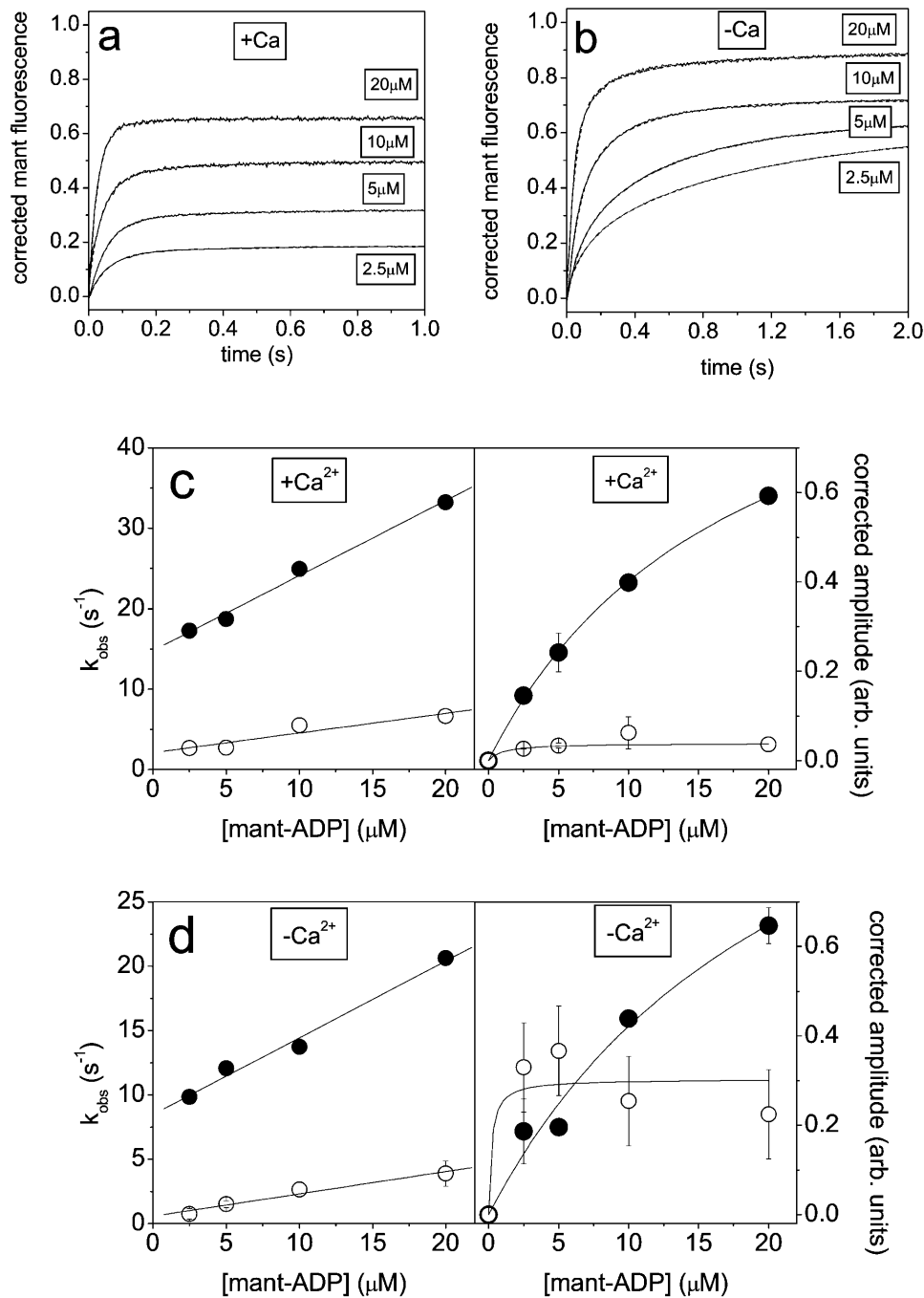
FIGURE 3 The binding of mant-ADP to scHMM in the presence and absence of calcium. The mant-fluorescence changes on mixing scHMM (0.5 μM) with mant-ADP (2.5–20 μM) in the presence (*a*), or absence (*b*), of calcium at 20 mM KCl. The mant-intensities were corrected using $F_{corr} = (F_m - F_i)/[mant]$, where F_m and F_i are the measured and initial intensities. Double-exponential fits are presented as dashed lines in the figure. The mant-ADP dependence of k_{obs} and amplitudes in the presence, *c*, and absence, *d*, of calcium. Filled and empty circles show the data obtained for the fast and slow phase, respectively. (*c*) +Ca: linear fits to k_{obs} values gave slopes of 9×10^5 $M^{-1}s^{-1}$ and 2.4×10^5 $M^{-1}s^{-1}$, with intercepts of 15 s^{-1} and 2 s^{-1}. Hyperbola fits to the amplitudes gave $K_{0.5}$ of 17.9 μM and <2 μM and A_{max} of 1.1 and 0.05. (*d*) −Ca: slopes were 6×10^5 $M^{-1}s^{-1}$ and 2×10^5 $M^{-1}s^{-1}$ with intercepts of 8.5 s^{-1} and 1 s^{-1}. Hyperbola fits to the amplitudes gave $K_{0.5}$ of 20 μM and <2.5 μM, and A_{max} of 1.2 and 0.3.

detected in these experiments, the maximum amplitudes indicate that besides the ~15–20% of unregulated scHMM, 6% of the heads are *off* and most of the heads (~74–79%) are *on* in the absence of ADP. At 100 mM KCl the presence of *off* heads was not detected in the presence of calcium previously—which suggests that the decrease of the ionic strength had only a small effect on the *on-off* equilibrium.

In the absence of calcium (Fig. 3 *d*) k_{obs} vs. [mant-ADP] plots were linear and gave apparent second-order binding constants (k_{-6}/K_7) of 6×10^5 $M^{-1}s^{-1}$ and 2×10^5 $M^{-1}s^{-1}$

for the fast and slow phases, respectively, similar to the values found in the presence of calcium. The intercept (k_{+6}) was 8.5 s^{-1} in the fast phase and <1 s^{-1} but not well-determined for the slow phase. Hyperbolic analysis of the amplitudes indicated that half-saturation occurred at ~20 μM mant-ADP for the faster phase, which gave an estimation of K_6K_7 for the *on* heads. In the slower phase the half-saturation mant-ADP concentration was 2.5 μM, giving an upper limit of K_6K_7 for the *off* heads. Hyperbola fits gave maximum amplitudes of 1.3 for the faster phase and 0.3 for the slower

one. These maximum amplitudes suggest that approximately one-third of the scHMM heads were *off* in the absence of calcium, i.e., ~67% of the heads were *on*, when correction was made for unregulated heads. A similar contribution of the *on* heads were determined at 100 mM KCl (64%), which indicates that the change of ionic strength has little effect on the *on-off* equilibrium in the absence of calcium and ADP.

The dissociation equilibrium constant of mant-ADP for scHMM (K_6K_7) at 20 mM KCl can be estimated by calculating the ratio of the dissociation rate constants (k_{+6}; Fig. 1) to the second-order binding constants (k_{-6}/K_7; Fig. 3). The affinity (K_6K_7) of mant-ADP for the scHMM *on* heads is determined from the fast phase to be ~14–21 μM at 20 mM KCl, in agreement with the half-saturation mant-ADP concentrations (18 μM from Fig. 3 *c* and 20 μM from Fig. 3 *d*) for the faster phase in mant-ADP binding experiments and similar to that measured at 100 mM KCl (15 μM; see Table 1.) (Nyitrai et al., 2002). For the *off* heads a similar calculation gave dissociation equilibrium constant of ~0.1 μM at 20 mM KCl, 140–210× tighter than that determined for the *on* heads. This value for K_6K_7 is in agreement with the half-saturation mant-ADP concentration determined for the slow phases in mant-ADP binding experiments (Fig. 3, *c* and *d*).

NB Plots of k_{obs} for fast and slow phase are similar +/− Ca, validating that the properties of the *on* and *off* states are independent of calcium but the occupancy of the two states varies with calcium.

The ionic strength dependence of the sedimentation of scHMM

Previous studies have shown that the sedimentation velocity of scHMM is sensitive to the conformations of scHMM and is calcium sensitive (Stafford et al., 2001). In the absence of calcium scHMM adopts a compact structure leading to fast sedimentation. In the presence of calcium, the sedimentation was slower than in EGTA due to a more extended conformation attributed to the independent rotation of the two heads. To corroborate the conclusions from kinetic experiments we used the method of analytical ultracentrifugation to determine the sedimentation of scHMM over a range of ionic strengths in either the presence or absence of calcium and ADP. The results obtained in these experiments are shown in Fig. 4. The appearance of a single peak at each ionic strength (Fig. 4 *a*) suggests that the *on* and *off* conformations of the scHMM are in a rapid equilibrium during the time course of the sedimentation experiment. This conclusion is in agreement with the rapid kinetic results (Nyitrai et al., 2002). The peaks are not single Gaussians since the scHMM preparation consists of a nearly equal ratio of short and long scHMM molecules differing in their tail portion by 20 nm. The peak value reflects the weight average value for the mixture. A reduction in ionic strength results in a faster sedimentation of scHMM under all conditions. The ionic strength dependence of the sedimentation peaks position in the presence or absence of ADP is shown in Fig. 4, *b* and *c*. The dependence of s_{peak} on the square root of ionic strength is almost linear for the data in the presence of both ADP and calcium (Fig. 4 *b*). The identical line is drawn on Fig. 4 *c* to aid comparison between the two data sets.

If ADP is bound to scHMM at low salt in the presence of calcium, the sedimentation is slower than that in the absence of calcium (Fig. 4, *a* and *b*). As the salt concentration is increased, this difference is reduced and disappears at ionic strengths >0.2 M. This is consistent with loss of the *off* state at higher ionic strengths. In the absence of ADP, calcium has little effect on the sedimentation at any ionic strength (Fig. 4 *c*), consistent with the *off* state requiring the presence of nucleotide.

At both 100 and 20 mM NaCl the binding of ADP to scHMM shifted the peak positions toward greater values, indicating a more compact structure, in the absence of calcium but not in its presence (Fig. 4 *b*). This is consistent with the kinetic data which shows that in the absence of calcium ADP addition results in a shift toward the more compact, faster sedimenting *off* state. In the presence of calcium the addition of ADP has little effect on the sedimentation (Fig. 4, *b* and *c*). This is consistent with the kinetic analysis where the system is substantially in the *on* state in the presence of calcium, independent of the presence of ADP, and independent of ionic strength. The salt concentrations in sedimentation and kinetic experiments were adjusted with NaCl and KCl, respectively. We repeated the rapid kinetic measurements in the presence of NaCl and the results showed that the rate constants for mant-ADP dissociation from scHMM were independent of the nature of the salt at either 20 mM salt or 100 mM salt, and in either the presence or absence of calcium.

TABLE 1 The comparison of kinetic rate and equilibrium binding constants determined experimentally at 20 mM and 100 mM KCl for the *on* and *off* conformations of scHMM heads

Conditions	Parameter	Units	Value		
			^{on}HMM	^{off}HMM	scS1*
100 mM KCl	k_{-6}/K_7	10^6 M^{-1}s^{-1}	1	0.5–0.8	1.5
	k_{+6}	s^{-1}	15	0.3–0.7	17
	K_6K_7	μM	15	1	11
20 mM KCl	k_{-6}/K_7[†]	10^6 M^{-1}s^{-1}	0.6–0.9	0.2–0.3	–
	k_{+6}	s^{-1}	12.5[‡]	0.02–0.03	12.5[‡]
	K_6K_7[§]	μM	15–20	0.1	–

The data at 100 mM KCl is from the previous work (Nyitrai et al., 2002).
*The data for scS1 were cited from Kurzawa-Goertz et al. (1998).
[†]From mant-ADP binding experiments.
[‡]From mant-ADP dissociation from scS1 experiments (Fig. 1). The intercepts in mant-ADP binding plots were in agreement with these data giving 8.5–15 s^{-1} and less than ~1 s^{-1} for the *on* and *off* forms, respectively.
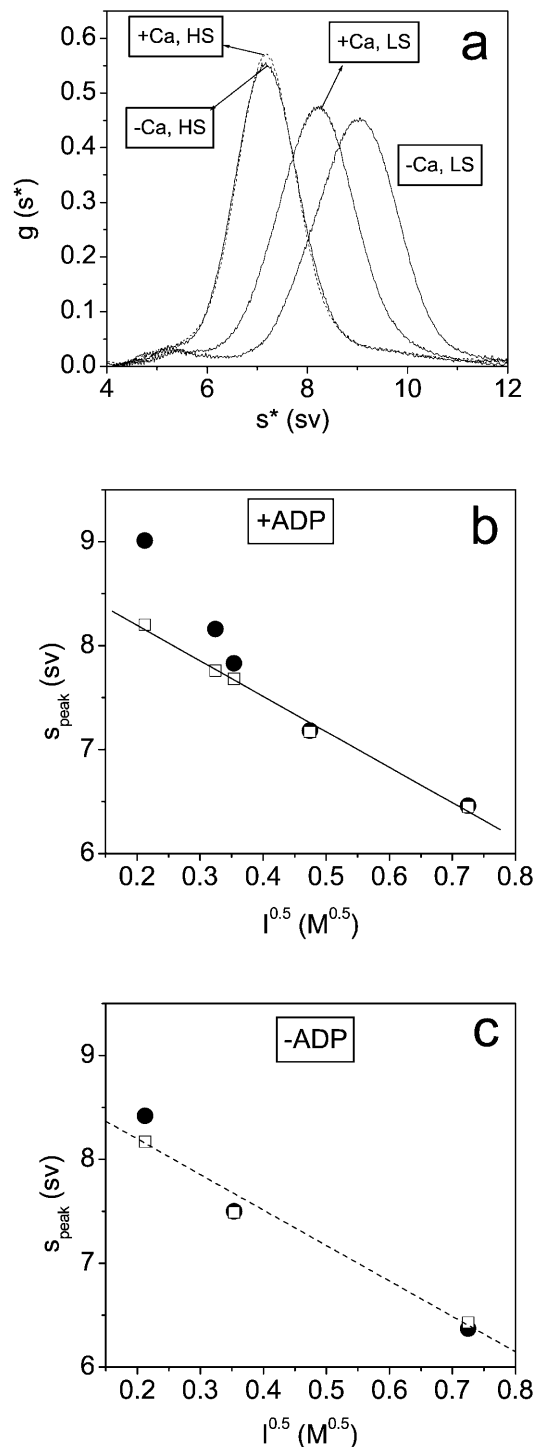[§]Calculated as $k_{+6}/k_{-6}/K_7$.

The ionic strength dependence of the kinetics of the dissociation of calcium from scHMM in the absence of nucleotides

The affinity of the calcium for scHMM depends on both the binding and dissociation kinetics. The determination of the binding of calcium and its dissociation in the presence of ADP was not possible as these processes are too fast to be measured in a stopped-flow experiment. The kinetics of calcium release in the absence of ADP, however, proved to be slower and could be determined by monitoring *Trp* fluorescence (Jackson and Bagshaw, 1988b; Nyitrai et al., 2002). As these two studies were carried out on different scallop species the direct comparison of the data obtained at 20 mM KCl ($25\ s^{-1}$ from Jackson and Bagshaw, 1988b) and at 100 mM KCl ($75\ s^{-1}$ from Nyitrai et al., 2002) is not appropriate. Therefore, in this study experiments were carried out at different KCl concentrations (20 mM, 60 mM, 100 mM, and 500 mM) using *Trp* fluorescence to provide information regarding the ionic strength dependence of the calcium release step. When scHMM (0.5 μM) and calcium (10 μM) was mixed with a large excess of EGTA (500 μM) the fluorescence of *Trp* decreased by ~3% regardless of the ionic strength. The traces (not shown) were single exponential and gave apparently KCl-independent k_{obs} values between $50\ s^{-1}$ and $80\ s^{-1}$.

The displacement of ADP with ATP

It was shown previously that only one of the scHMM heads could bind ADP in the absence of calcium at 100 mM KCl. This property of scHMM was observed when ADP was displaced with ATP and the changes in *Trp* fluorescence were recorded. The appearance of a fast component showed that even at 40 μM ADP (~20× of the $K_6 K_7$) approximately half of the heads bound ATP very quickly, indicating that they did not bind ADP. To gain further information about this specific behavior of scHMM the ADP displacement experiments were repeated at lower KCl concentrations (0 mM or 20 mM KCl) where the binding of ADP to scHMM is expected to be tighter. In the absence of ADP, the fluorescence transients were single exponential and gave amplitudes of 2.5% and 3.6% at 0 mM and 20 mM KCl, respectively (Fig. 5, *a* and *b*). These values are a factor of 2–3 smaller than the one (7.5%) measured at 100 mM KCl (Fig. 5 *c*). The resolved k_{obs} values were $180\ s^{-1}$, $210\ s^{-1}$, and $250\ s^{-1}$ at 0 mM KCl, 20 mM KCl, and 100 mM KCl, respectively, and were attributed to the fast binding of ATP to the nucleotide pocket. When scHMM was incubated with 15 μM ADP (more than 10× that of the $K_6 K_7$, Table 1) before mixing with ATP, the traces were double exponential. The slow phase in these transients represents scHMM heads with bound ADP, which must dissociate from the heads before ATP binds. The amplitude of these slow components were <1%, which is consistent with the fact that the

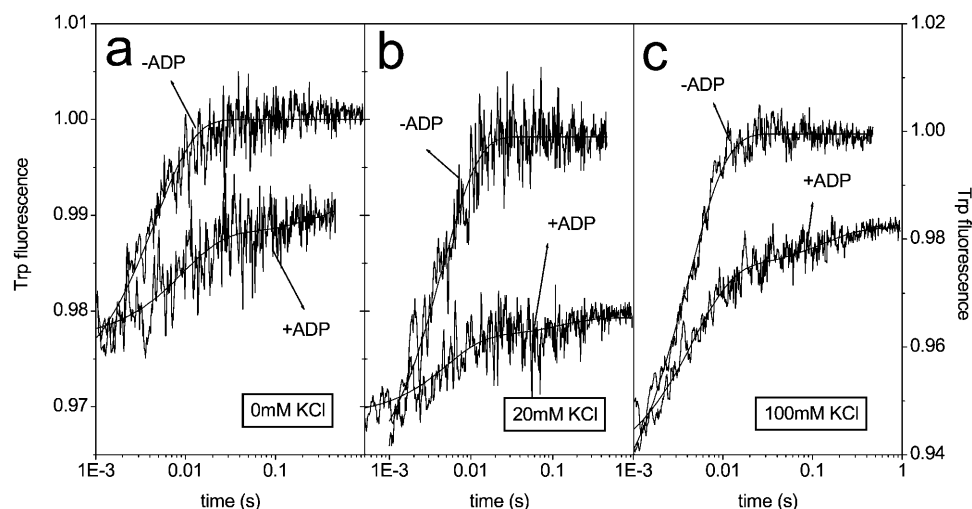FIGURE 4 The ionic strength dependence of the sedimentation of scHMM. (*a*) Sedimentation results in the presence of 100 μM ADP with and without 100 μM calcium (as indicated) at 20 mM NaCl (*LS*) and at 200 mM NaCl (*HS*). (*b*) The dependence of sedimentation on √(ionic strength) in 100 μM ADP with a best fit line drawn through the data in the presence of calcium. (*c*) Data in the absence of nucleotides with the line reproduced from *b* to aid comparison. The peak positions are shown in the presence (*empty squares*) and absence (*filled circles*) of calcium (100 μM). Protein concentrations were typically in the range 0.1–1.0 mg/ml. No concentration dependence of the sedimentation patterns was seen, indicating the absence of any reversible aggregation.

FIGURE 5 Tryptophan signals on the displacement of ADP by ATP in the absence of calcium. Scallop HMM (0.5 μM) and ± 7.5 μM ADP were mixed with ATP (300) at 0 mM (*a*), 0 mM (*b*), and 100 mM (*c*) KCl. In the absence of ADP the traces were single exponential with amplitudes and k_{obs} values of 2.5%, 3.0%, and 7.5%, and 180 s^{-1}, 210 s^{-1}, and 250 s^{-1} at 0 mM, 20 mM, and 100 mM KCl, respectively. In the presence of ADP, the traces were double exponential. The fast phases gave amplitudes and k_{obs} values of 1.1%, 1%, and 3.7%, and 160 s^{-1}, 220 s^{-1}, and 220 s^{-1}, respectively. The amplitude of the slow phase was small ($<1\%$) at all ionic strengths, and determination of k_{obs} values was not possible.

fluorescence changes are similar for the binding of ATP and ADP, and thus the replacement of ADP with ATP contributes little to the total fluorescence change. Fast phases were observed in the presence of ADP regardless of the KCl concentration (Fig. 5). The resolved k_{obs} values were 160 s^{-1}, 220 s^{-1}, and 220 s^{-1} at 0 mM, 20 mM, and 100 mM KCl, similar to those measured in the absence of ADP. The fast phases therefore represent the scHMM heads with no bound ADP. The amplitudes of these fast phases were 1.1%, 1.0%, and 3.7% at 0 mM, 20 mM, and 100 mM KCl, respectively, with 44%, 28%, and 50% of the fast phase measured in the absence of ADP. Although the error attributed to the determination of the amplitudes is greater at lower ionic strength (0 mM or 20 mM KCl), these values are compatible with the observation that approximately half of the scHMM cannot bind ADP in the absence of calcium.

DISCUSSION

The data present here are all consistent with our previous proposal (Nyitrai et al., 2002) that scHMM exists in two conformations *off* and *on*, and that the equilibrium position between the two conformations is modulated by both calcium and ADP. In addition, we show here that the equilibrium is also influenced by ionic strength suggesting a major role for ionic interactions in stabilizing the *off* conformation. We have presented two lines of evidence to support this view from kinetic and sedimentations studies.

The kinetic evidence is based on the observation that the affinity of scHMM for mant-ADP ($K_6 K_7$) is calcium dependent, and that this is due to a calcium-dependent rate constant for ADP release (k_{+6}). Analysis of the k_{obs} for mant-ADP release as a function of calcium and ionic strength were interpreted in terms of the model shown in Scheme 2 and the results of this analysis are summarized in Tables 1 and 2.

The calcium dependence of the k_{obs} for ADP displacement shows the classic behavior for a cooperative switching

system where the binding of two calcium ions are required to switch between the high and low ADP affinity states (Fig. 1 *c*). This cooperative switching behavior is apparent at all ionic strengths <0.2 M; above this ionic strength, the switching is no longer apparent and the scHMM is in the low ADP affinity *on* state independent of calcium. The calcium affinity (0.78 to 1.8 μM from 0.1 to 0.02 M KCl) and the Hill coefficient (1.9–2.2) show little ionic strength dependence within the limits of the measurements. The calcium and salt dependence of the ADP release rate constant can be explained by the model shown in Scheme 2. The detailed interpretation in terms of Scheme 2 depends upon the assumption that behavior of scS1 provides a reasonable model for the intrinsic salt dependence of the ADP release rate constant from the *scHMM*^{on}. The k_{obs} for ADP release from S1 showed only a twofold reduction as the [KCl] was reduced from 0.5 M to 0 M, indicating a minor dependence upon ionic strength. In contrast, the scHMM showed an almost 10-fold reduction in the presence of calcium and a 1000-fold reduction in the absence of calcium. Both reductions can be an indication of increased occupancy of the *off* state as the ionic strength is reduced.

TABLE 2 The summary of equilibrium association constants defining the equilibrium between the *on* and *off* conformations of scHMM in the presence and absence of calcium

Conditions	Parameter	Value	
		$+Ca^{2+}$	$-Ca^{2+}$
100 mM KCl	$K_{eq}^{ADP}*$	15 (94% *on*)	10^{-2} ($<1\%$ *on*)
	K_{eq}†	v. large ($>99\%$ *on*)	~ 2 ($\sim 67\%$ *on*)
20 mM KCl	$K_{eq}^{ADP}*$	2 (67% *on*)	2×10^{-3} ($<0.1\%$ *on*)
	K_{eq}†	20 ($>94\%$ *on*)	~ 2 ($\sim 67\%$ *on*)

*Data from the analysis of mant-ADP replacement with ATP experiments.
†Estimations from the amplitudes measured in mant-ADP binding experiments. $K_{eq} = [on]/[off]$, in the absence (K_{eq}) or presence (K_{eq}^{ADP}) of ADP. The contribution of *on* heads to the total scHMM population was calculated from K_{eq} as: $on/(on + off) = K_{eq}/(1 + K_{eq})$.

Interpretation of the data terms of Scheme 2 and Eqs. 2 and 3 suggests that the reduction in the k_{obs} values with reduced calcium concentrations and reduced ionic strength is due to a combination of increasing occupancy of the *off* conformation and the lower value of $^{off}k_{+6}$ in the *off* state. If $^{off}k_{+6}$ has the same low salt dependence as the k_{+6} value for scS1 (twofold) then the limiting value of $^{off}k_{+6}$ is 0.01 s^{-1}. It remains possible, however, that ADP is not released at all from the *off* state, and that $^{off}k_{+6}$ is zero. In this case, Eq. 2 becomes

$$k_{obs} = {}^{on}k_{+6}\alpha[scHMM]_{total} = {}^{on}k_{+6}K_{eq}[scHMM]_{total}/(1+K_{eq})$$
(4)

Either interpretation of the model suggests that the effects of both calcium and salt are primarily on the equilibrium between the *on* and *off* states in the presence of ADP, with both low calcium and low salt favoring the *off* state. The influence of low calcium is reduced at high salt concentrations and reciprocally the influence of salt is diminished in the presence of calcium. These effects are only clearly seen in the presence of ADP.

The conformation of the *on* and *off* states can also be followed by sedimentation studies. Previous work has shown that in the presence of ADP or ATP analogs but no calcium, scHMM takes up a more compact structure and sediments faster than in the state induced by calcium (Stafford et al., 2001). We show here that in the presence of ADP, the calcium-induced difference in sedimentation is greater at low salt concentration and disappears at ionic strengths exceeding 0.2 M (Fig. 4 *c*). This is consistent with the estimates of the equilibrium between *on* and *off* states in Table 2. Scallop HMM sediments always as a single peak at different salt concentrations indicating that the *on* and *off* conformations are in an ionic strength-dependent equilibrium. There is also a marked salt dependence of sedimentation independent of the *on/off* equilibrium position shown most markedly in the −ADP +Ca data which is expected to be >95% *on* at all salts conditions except the very lowest. The relationship between S and $I^{0.5}$ was almost linear under these conditions and ADP had little effect, except at the lowest ionic strengths used—again consistent with the K_{eq} values in Table 2.

This marked ionic strength dependence of sedimentation properties under conditions where the scHMM is expected to be predominantly *on* suggest that the state cannot be associated with precise structural states. It is consistent with significant conformational heterogeneity in the *on* state which is sensitive to the ionic strength. This may be expected for the *on* state which is thought to be one in which the two heads have independent movement, and therefore disorder, around the head-S2 junction. Such heterogeneity is not expected for an *off* state in which the two heads are docked together onto the myosin tail. The marked salt-dependent behavior of the sedimentation of the *on* state caused by changes in the conformational heterogeneity may be larger than subtle changes in the *on/off* equilibrium under some

conditions. This precludes a more detailed comparison of the sedimentation and kinetic data. The overall conclusion is that both the kinetic and sedimentation data are consistent with a dynamic Ca-dependent equilibrium between two primary conformations of scHMM with the equilibrium position being influenced by salt and nucleotide. Low calcium, ADP, and low salt all favor the *off* conformation. The kinetic data allow the best definition of the equilibrium constant in the presence of ADP at salt concentration <0.1 M. No *off* state is detected at salts >0.2 M independent of calcium, and little *on* state is detected at low salt in the absence of Ca.

The evidence for *on* and *off* states in the absence of ADP is not as clear in the presence of ADP and relies on estimates of the relative amplitudes of the two phases in the mant-ADP binding data which are Ca dependent. This interpretation in terms of two populations of *on* and *off* states requires that the two states are kinetically distinct populations on the timescale of mant-ADP binding and therefore the *on/off* equilibration must be slower than the rate of mant-ADP binding, i.e., in the absence of ADP the *on/off* equilibration is slower than in the presence of ADP. In support of a difference in the equilibrium behavior in the absence of nucleotide is the observation that both the sedimentation and the mant-ADP binding data are consistent with a much smaller influence of salt on the *on/off* equilibrium in the absence of nucleotide.

All of the data presented here are consistent with our previous observation that the HMM^{off} binds only a single ADP. The *off* state therefore must have an asymmetric structure as reported for smHMM in both kinetic studies (Berger et al., 2001) and in EM images of smHMM and myosin (Wendt et al., 2001). There is nothing in our sedimentation data which rules out the type of structure reported by Wendt et al. (2001) for smHMM, but other asymmetric structural models remain possible for scHMM. Whatever the structure of the *off* state, it must account for the observation that only a single head can bind ADP.

A significant observation is that the *off* state, discussed here, is a characteristic of regulated myosins, and requires the interaction between two heads of myosin. Sedimentation data are consistent with a model where the two heads interact with each other and form a rigid structure. In case of scallop HMM and myosin, calcium disrupts the interaction between the heads which become mobile and can enter the ATPase cycle (Stafford et al., 2001).

The nature and dynamics of the *off* conformation

Atomic models from crystallographic studies suggest that there is direct coupling between the conformation of the structural element known as switch II which contacts the P_i of ATP, the converter domain and the orientation of the light-chain-binding domain (or tail or lever arm). For convenience this overall conformational switch is here referred to as the switch II *open/closed* conformation change.

The structures determined in different nucleotide states (Fisher et al., 1995; Smith and Rayment, 1996; Dominguez et al., 1998; Geeves and Holmes, 1999; Houdusse et al., 1999; Bauer et al., 2000) suggested that hydrolysis of ATP on myosin only happens in the *closed* conformation of the motor domain, while the power stroke and the associated P_i and ADP release require the structure to return to the *open* conformation. If the *off* state involves a ''docking'' of one head of HMM onto the partner head (as in Wendt et al., 2001), or one or both heads onto S2, this would restrict the ability of the head to go through the major conformational changes associated with the *open/closed* tail swing and therefore would produce an inhibition of the cycle. For some myosins, notably smooth muscle myosin, there is an additional movement of the light-chain-binding domain (LCBD) on binding and release of ADP (Whittaker et al., 1995; Jontes et al., 1995). The potential for a direct communication between the regulatory LCBD and nucleotide therefore clearly exists. Any change in the LCBD which restricts the movement of the LCBD relative to the converter domain therefore has the potential to influence the *open-closed* transition and ATP hydrolysis and the overall cycle.

REFERENCES

Bagshaw, C. R., and D. R. Trentham. 1974. The characterization of myosin-product complexes and of product-release steps during the magnesium ion-dependent adenosine triphosphatase reaction. *Biochem. J.* 141:331–349.

Bauer, C. B., H. M. Holden, J. B. Thoden, R. Smith, and I. Rayment. 2000. X-ray structures of the apo and MgATP-bound states of *Dictyostelium discoideum* myosin motor domain. *J. Biol. Chem.* 275:38494–38499.

Berger, C. E., P. M. Fagnant, S. Heizmann, K. M. Trybus, and M. A. Geeves. 2001. ADP binding induces an asymmetry between the heads of unphosphorylated myosin. *J. Biol. Chem.* 276:23240–23245.

Chantler, P. D., and A. G. Szent-Györgyi. 1980. Regulatory light-chains and scallop myosin. Full dissociation, reversibility and co-operative effects. *J. Mol. Biol.* 138:473–492.

Dominguez, R., Y. Freyzon, K. M. Trybus, and C. Cohen. 1998. Crystal structure of a vertebrate smooth muscle myosin motor domain and its complex with the essential light chain: visualization of the pre-power stroke state. *Cell.* 94:559–571.

Ellison, P. A., Z. S. DePew, and C. R. Cremo. 2002. Both heads of tissue-derived smooth muscle heavy meromyosin bind to actin in the presence of ADP. *J. Biol. Chem.* 278:4410–4415.

Fisher, A. J., C. A. Smith, J. B. Thoden, R. Smith, K. Sutoh, H. M. Holden, and I. Rayment. 1995. X-ray structures of the myosin motor domain of *Dictyostelium discoideum* complexed with MgADP. BeFx and MgADP. AlF4. *Biochemistry.* 34:8960–8972.

Geeves, M. A., and K. C. Holmes. 1999. Structural mechanism of muscle contraction. *Annu. Rev. Biochem.* 68:687–728.

Harrison, S. M., and D. M. Bers. 1987. The effect of temperature and ionic strength on the apparent Ca-affinity of EGTA and the analogous Ca-chelators BAPTA and dibromo-BAPTA. *Biochim. Biophys. Acta.* 925:133–143.

Houdusse, A., V. N. Kalabokis, D. Himmel, A. G. Szent-Györgyi, and C. Cohen. 1999. Atomic structure of scallop myosin subfragment S1 complexed with MgADP: a novel conformation of the myosin head. *Cell.* 97:459–470.

Jackson, A. P., and C. R. Bagshaw. 1988a. Kinetic trapping of intermediates of the scallop heavy meromyosin adenosine triphosphatase reaction revealed by formycin nucleotides. *Biochem. J.* 251:527–540.

Jackson, A. P., and C. R. Bagshaw. 1988b. Transient-kinetic studies of the adenosine triphosphatase activity of scallop heavy meromyosin. *Biochem. J.* 251:515–526.

Jontes, J. D., E. M. Wilson-Kubalek, and R. A. Milligan. 1995. A 32° tail swing in brush border myosin I on ADP release. *Nature.* 378:751–753.

Kalabokis, V. N., and A. G. Szent-Györgyi. 1997. Cooperativity and regulation of scallop myosin and myosin fragments. *Biochemistry.* 36: 15834–15840.

Kurzawa-Goertz, S. E., C. L. Perreault-Micale, K. M. Trybus, A. G. Szent-Györgyi, and M. A. Geeves. 1998. Loop I can modulate ADP affinity, ATPase activity, and motility of different scallop myosins. Transient kinetic analysis of S1 isoforms. *Biochemistry.* 37:7517–7525.

Nyitrai, M., A. G. Szent-Györgyi, and M. A. Geeves. 2002. Kinetic model of the cooperative binding of calcium and ADP to scallop heavy meromyosin. *Biochem. J.* 365:19–30.

Smith, C. A., and I. Rayment. 1996. X-ray structure of the magnesium (II).ADP.vanadate complex of the *Dictyostelium discoideum* myosin motor domain to 1.9 Å resolution. *Biochemistry.* 35:5404–5417.

Stafford, W. F., M. P. Jacobsen, J. Woodhead, R. Craig, E. O'Neall-Hennessey, and A. G. Szent-Györgyi. 2001. Calcium-dependent structural changes in scallop heavy meromyosin. *J. Mol. Biol.* 307:137–147.

Szent-Györgyi, A. G., V. N. Kalabokis, and C. L. Perreault-Micale. 1999. Regulation by molluscan myosins. *In* Muscle Physiology and Biochemistry. S. Imai, M. Endo, and I. Ohtsuki, editors. Kluwer Academic Publishers Group. pp.55–62.

Trybus, K. M. 1991. Regulation of smooth muscle myosin. *Cell Motil. Cytoskeleton.* 18:81–85.

Wells, C., K. E. Warriner, and C. R. Bagshaw. 1985. Fluorescence studies on the nucleotide- and Ca^{2+}-binding domains of molluscan myosin. *Biochem. J.* 231:31–38.

Wendt, T., D. Taylor, K. M. Trybus, and K. Taylor. 2001. Three-dimensional image reconstruction of dephosphorylated smooth muscle heavy meromyosin reveals asymmetry in the interaction between myosin heads and placement of subfragment 2. *Proc. Natl. Acad. Sci. USA.* 98:4361–4366.

Whittaker, M., E. M. Wilson-Kubalek, J. E. Smith, L. Faust, R. A. Milligan, and H. L. Sweeney. 1995. A 35-A movement of smooth muscle myosin on ADP release. *Nature.* 378:748–751.